SYNTHESIS, MOLECULAR STRUCTURE AND DYNAMIC BEHAVIOUR OF THE CHIRAL CLUSTER $(\mu\text{-H})_4Ru_4(CO)_9(HC(PPh_2)_3)$

A. A. Bahsoun, and J. A. Osborn

Laboratoire de Chimie Inorganique Moléculaire et de Catalyse (ERA-C.N.R.S. n° 721).

J.-P. Kintzinger

Laboratoire de Chimie Organique Physique (ERA-C.N.R.S. n° 265).
Institut Le Bel, Université Louis-Pasteur, 4, rue Blaise-Pascal, 67000 Strasbourg (France).

P. H. Bird, and U. Siriwardane

Department of Chemistry, Concordia University, Montreal, Quebec, Canada H3G IM8.

Received September 19, 1983.

RÉSUMÉ. — Nous décrivons la synthèse et l'étude du comportement dynamique en solution de $(\mu\text{-H})_4Ru_4(CO)_9(HC(PPh_2)_3)$. La détermination structurale par rayons X montre que ce cluster est chiral, l'asymétrie résultant d'un déploiement hélicoïdal des groupes phényls du ligand tripode.

ABSTRACT. — The synthesis and study of the dynamic behaviour of $(\mu\text{-H})_4Ru_4(CO)_9(HC(PPh_2)_3)$ are described. The X-ray structural determination shows this cluster to be chiral, the asymmetry arising from a helical array of phenyl groups on the tripod ligand.

Introduction

In a recent study [1] we showed that the ligand $HC(PPh_2)_3$ (hereafter *tripod*) could serve to complex three metal atoms in a triangular array e. g. "cap" a triangular face of clusters such as $M_4(CO)_{12}$ (M = Co, Rh). We found that the analogous complex, $H_4Ru_4(CO)_{12}$ also reacted [2] smoothly with tripod to yield the complex $H_4Ru_4(CO)_9$(tripod). The spectroscopic data (IR, NMR) of this molecule, although consistent with a capped structure, showed some unexpected features which we decided to investigate further.

There have been several structural and spectroscopic studies of phosphine substituted derivatives of $H_4Ru_4(CO)_{12}$. Interest has mainly focused on the position of the hydride ligands on the cluster surface and the mechanism of their intramolecular site exchange. Two structural forms for the M_4H_4 *core* have been established which are shown schematically below.

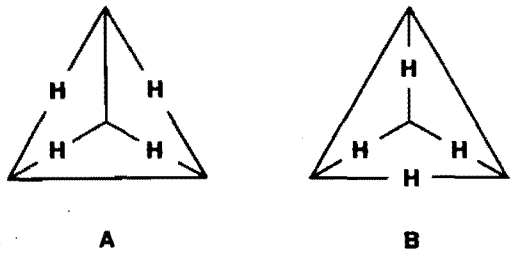

Scheme I

Core structure *A*, (D_{2d} symmetry) has hydride ligands bridging four edges of the tetrahedron so that two opposite edges remain vacant. This has been found for $(\mu\text{-H})_4Ru_4(CO)_{12}$ [3], $(\mu\text{-H})_4Ru_4(CO)_{11}P(OMe)_3$ [4], and $(\mu\text{-H})_4Ru_4(CO)_{10}(PPh_3)_2$ [3]. Core structure *B* (C_s symmetry) has been established for both isomers [5, 6] of $(\mu\text{-H})_4Ru_4(CO)_{10}(Ph_2PCH_2CH_2PPh_2)$. Since the tripod ligand imposes facial substitution (assuming all phosphorus atoms are bound), we anticipated the limiting low temperature spectrum of the hydride region to show either a 2H : 2H pattern (*A*) or a 1H : 2H : 1H pattern (*B*). However four separate resonances are observed which prompted us to investigate in more detail the spectroscopy and carry out an X-ray diffraction analysis of this compound.

Experimental section

SYNTHETIC METHODS

The parent cluster $H_4Ru_4(CO)_{12}$ was synthesized following the method of Kaesz *et al.* [7]. The tripod ligand was prepared as described previously [1]. Elemental analysis were performed at the Service Central d'Analyses of the C.N.R.S. IR spectra were obtained in solution using 0.1 mm path length KCl cells with a Perkin-Elmer 597 spectrophotometer. NMR spectra were recorded on Cameca-250, Bruker WH 90 and Bruker WP 200-SY spectrometers.

$(\mu\text{-H})_4Ru_4(CO)_9(HC(PPh_2)_3)$. — $(\mu\text{-H})_4Ru_4(CO)_{12}$ (290 mg, 0.39 mmol) was dissolved in n-octane (80 ml) at 95-100°. A solution of $HC(PPh_2)_3$ (220 mg, 0.39 mmol) in toluene (20 ml) was added dropwise over 45 minutes with stirring. The initial deep yellow solution darkened to deep red during addition, and the solution was heated at 95° for a further 1 hour. The solution was vacuum evapora-

ted to dryness, the residue washed with hexane, and then with several 1 ml portions of cold toluene. Pure deep orange crystals of $H_4Ru_4(CO)_9(HC(PPh_2)_3)$ were obtained by recrystallisation from CH_2Cl_2 : hexane (1 : 2) (yield: 50-55%).

Crystals suitable for an X-ray study were obtained as $(\mu\text{-}H)_4Ru_4(CO)_9(HC(PPh_2)_3)$. CH_2Cl_2 by slow evaporation of a saturated solution of the complex in CH_2Cl_2.

The reaction can more conveniently be carried out by preparing $H_4Ru_4(CO)_{12}$ *in situ* by treatment of $Ru_3(CO)_{12}$ with hydrogen in refluxing cyclohexane for 2 hours. Formation of $H_4Ru_4(CO)_{12}$ can be followed by solution infrared analysis, and tripod added as above when this initial reaction was completed. Other experimental details are as described above.

IR (CH_2Cl_2). – ν_{CO} 2066(s), 2010(vs), 1995(vs), 1957(vw) and 1935(w) cm^{-1}. *^1H NMR* (CD_2Cl_2, 30°): (μ-H) τ 25.76(q, 4H, J_{P-H}) = 0.5 Hz); C_6H_5 τ 2.8-3.1(m, 30H). *$^{31}P\{^1H\}$* (CD_2Cl_2, 30°): +35.9 p.p.m. (vs. H_3PO_4, s, $\Delta\nu_{1/2}$ = 5 Hz). A sample of this complex *ca.* 35% enriched with ^{13}CO was made by direct exchange with ^{13}CO. *$^{13}C\{^1H\}$* (CD_2Cl_2, 30°): 196.8 p.p.m. (s, relative intensity ~6) and 191.7 p.p.m. (s, relative intensity ~3).

X-RAY DATA COLLECTION, STRUCTURE SOLUTION AND REFINEMENT

The crystallographic data are summarized in Table I: the following procedure was used. The space group was established by a preliminary study of Weissenberg and precession photograph of the three zero and first levels. The systematic absences on $h\ 0\ l$, $h+l=2n+1$ and on $0\ k\ 0$, $k=2n+1$ uniquely define $P2_1/n$ [a non-standard setting of $P2_1/c$ (No. 14)]. The crystal was aligned on a Picker Nuclear FACS-1 single crystal diffractometer, and the accurate unit cell and orientation matrix were determined by least-squares refinement using the setting angles for 30 automatically centered reflections. The chosen reflections were randomly distributed in reciprocal space in the range $15 < 2\theta < 30°$. Intensity data were collected using a reflection profile analysis for background determination [8]. Three reference reflections were remeasured every 50 cycles: random variations of less than 3% were observed.

The following formulae were applied:

$$I = N - B\,t_s/t_b, \qquad \sigma(I) = [N + B(t_s/t_b)^2]^{1/2},$$

$$Lp = \frac{(\sin 2\theta_s)(\cos^2 2\theta_m + 1)}{(\cos^2 2\theta_s + \cos^2 2\theta_m)}.$$

Here, I is the net intensity derived from a count N measured during a line of t_s, B is the estimated background in time t_b, Lp is the Lorentz-polarization correction, where $2\theta_m$ and $2\theta_s$ are the diffraction angles at the monochromator (graphite) and sample, respectively. The linear absorption coefficient for Mo K_α radiation is 14.20 cm^{-1} and estimated transmission factors range from 0.85 to 0.90: no absorption correction was applied.

The positions of the 4 ruthenium atoms were deduced from an E-map after statistical phasing of 173 reflections by Multan. A serie of structure factor calculations and difference Fourier synthesis revealed the remaining non-hydrogen atoms, including a molecule of CH_2Cl_2. The structure was refined isotropically for 7 cycles and then partly anisotropically (phenyl rings isotropic) for 5 cycles using the block diagonal approximation (shifts multiplied by 0.6). The discrepancy indices at this point were: $R_F = 0.047$ and $R_{WF} = 0.071$. A difference Fourier synthesis using 1355 reflections having $\sin\theta/\lambda < 0.35$ revealed peaks for essentially all the hydrogen atoms. In particular the 4 cluster hydrides were very distinct, with peak heights ranging from 0.6 to 0.8 $e^-/Å^3$. Refinement was continued for a further 5 cycles. The cluster H atoms were refined with isotropic thermal parameters, while all others were placed in calculated positions, and given the same isotropic thermal parameters as the carbon to which they were attached. A final difference synthesis showed only random residual density less than 0.5 $e^-/Å^3$.

Table I. – Data collection and refinement.

a	17.046(2) Å
b	16.347(5) Å
c	17.870(3) Å
β	87.02(1)°
Space group	$P2_1/n$
Mol Wt	1228.81
Z	4
u	4972.8 $Å^3$
ρ calcd	1.755 $g.cm^{-3}$
ρ obsd	1.76(1) $g.cm^{-3}$ (by flotation)
Radiation	Mo K_α (λ = 0.71069 Å, α_1/α_2 doublet not resolved)
Monochromator	Highly oriented graphite, $2\theta_{002} = 12.1°$
Crystal-detector dist	25 cm
Detector	Scintillation counter and pulse height analyser set for 100% of MoK α peak
Attenuators	Ni foil, when counting rate exceeded 10^4 counts, s^{-1}
Take-off-angle	3.0°
Dectector aperture	4 × 4 mm
Scan type	Coupled θ(cryst)-2θ (detector), 2.0° min^{-1}
Scan base width	1.4°
Scan length	$\Delta(2\theta) = [1.4 + (0.692 \tan\theta)]°$, beginning 0.7° below the predicted peak
Rotation axis	[0 1 0]
Reflections measured	$\pm h, +k, +l$
Min and max 2θ	3.5, 40.0°
Stds every 50 cycles	6 0 $\bar{2}$, 6 4 $\bar{6}$, 7 1 3
Variation	±3%, random
Number of reflections collected	4618
No. with $I > 3\sigma(I)$	2785
R_F	0.043
R_{wF}	0.066
GOF	1.02

Table II. -

Atom
Ru1
Ru2
Ru3
Ru4
H12
H13
H24
H34
C11
O11
C12
O12
C21
O21
C22
O22
C31
O31
C32
O32
C41
O41
C42
O42
C43
O43
CP
P1
C111
C112
C113
C114
C115
C116
C121

The dat
geometry c
PDP-8A m
System. St
Concordia
in the least

$\Sigma w(|F_o| -$

The disc
$R_{wF} = [\Sigma w$
$[\Sigma w(|F_o| -$
anomalous
final posit
observed a
parameters
available a

Crystal Da
nic spac
$c = 17.870$
fractometr
factors for
groups iso
not refine
$R_w = 0.056$

Table II. – Final fractional coordinates for $H_4Ru_4(CO)_9$ (tripod), CH_2Cl_2 with estimated standard deviations in parentheses.

Atom	x	y	z	Atom	x	y	z
Ru1	0.27911(5)	0.22349(6)	0.12165(5)	C122	0.3946(7)	0.4244(7)	−0.0441(6)
Ru2	0.15606(5)	0.11772(5)	0.06138(5)	C123	0.4130(8)	0.5081(8)	−0.0414(7)
Ru3	0.11530(5)	0.27728(5)	0.10892(5)	C124	0.3781(7)	0.5568(8)	0.0094(7)
Ru4	0.16580(5)	0.15596(6)	0.21982(5)	C125	0.3241(7)	0.5274(7)	0.0627(6)
H12	0.226(4)	0.154(4)	0.092(4)	C126	0.3053(6)	0.4430(6)	0.0618(6)
H13	0.203(5)	0.294(6)	0.123(5)	P2	0.20097(16)	0.15546(17)	−0.05821(15)
H24	0.124(6)	0.094(6)	0.153(5)	C211	0.1380(6)	0.1439(6)	−0.1362(6)
H34	0.098(4)	0.235(5)	0.192(4)	C212	0.0898(7)	0.0763(7)	−0.1345(6)
C11	0.3218(6)	0.3013(7)	0.1819(6)	C213	0.0431(8)	0.0572(8)	−0.1938(7)
O11	0.3513(5)	0.3493(5)	0.2196(5)	C214	0.0433(8)	0.1073(9)	−0.2533(7)
C12	0.3600(7)	0.1512(7)	0.1372(6)	C215	0.0894(7)	0.1735(8)	−0.2589(7)
O12	0.4115(5)	0.1055(5)	0.1444(5)	C216	0.1393(6)	0.1931(7)	−0.1993(6)
C21	0.1857(7)	0.0055(7)	0.0520(6)	C221	0.2859(6)	0.0969(7)	−0.0969(6)
O21	0.1963(6)	−0.0639(5)	0.0464(6)	C222	0.3370(7)	0.0580(7)	−0.0499(6)
C22	0.0517(7)	0.0981(6)	0.0482(6)	C223	0.4011(7)	0.0122(7)	−0.0782(7)
O22	−0.0150(4)	0.0833(4)	0.0409(4)	C224	0.4121(8)	0.0040(8)	−0.1541(7)
C31	0.0098(7)	0.2576(7)	0.1078(6)	C225	0.3630(8)	0.0405(8)	−0.2022(7)
O31	−0.0587(4)	0.2487(5)	0.1109(5)	C323	0.2200(7)	0.5413(8)	−0.1048(6)
C32	0.0977(6)	0.3789(7)	0.1601(6)	C226	0.3000(7)	0.0866(7)	−0.1731(6)
O32	0.0806(6)	0.4348(5)	0.1946(5)	P3	0.13912(16)	0.32149(17)	−0.01481(15)
C41	0.2072(6)	0.2231(7)	0.2919(7)	C311	0.0583(5)	0.3108(6)	−0.0797(5)
O41	0.2319(5)	0.2620(7)	0.3387(5)	C312	0.0020(6)	0.2518(7)	−0.0685(6)
C42	0.0794(6)	0.1156(8)	0.2789(6)	C313	−0.0616(7)	0.2483(7)	−0.1143(6)
O42	0.0293(5)	0.0879(5)	0.3149(5)	C314	−0.0710(7)	0.3035(7)	−0.1707(6)
C43	0.2330(7)	0.0705(8)	0.2379(7)	C315	−0.0149(7)	0.3642(7)	−0.1810(7)
O43	0.2746(6)	0.0155(7)	0.2472(6)	C316	0.0499(6)	0.3674(6)	−0.1384(6)
CP	0.2298(5)	0.2685(6)	−0.0601(6)	C321	0.1580(6)	0.4303(6)	−0.0321(5)
P1	0.31496(16)	0.28214(18)	0.00568(15)	C322	0.2117(6)	0.4577(7)	−0.0899(6)
C111	0.4017(6)	0.2441(6)	−0.0477(6)	C324	0.1723(8)	0.5946(8)	−0.0642(7)
C112	0.4665(7)	0.2273(7)	−0.0043(6)	C325	0.1190(8)	0.5697(8)	−0.0101(7)
C113	0.5362(8)	0.1962(8)	−0.0449(7)	C326	0.1112(7)	0.4864(7)	0.0075(6)
C114	0.5383(8)	0.1886(9)	−0.1180(8)	CL2	0.2243(4)	0.3017(4)	0.6157(5)
C115	0.4753(8)	0.2072(8)	−0.1612(7)	C1	0.2880(10)	0.3808(9)	0.6365(8)
C116	0.4075(7)	0.2350(7)	−0.1239(6)	CL1	0.3127(5)	0.3738(4)	0.7285(3)
C121	0.3391(6)	0.3915(6)	0.0076(5)				

The data collection, structure solution, refinement and various geometry calculations were all performed using programs run on a PDP-8A minicomputer using the NRC PDP-8E Crystal Structure System. Structure diagrams were prepared using ORTEP on the Concordia University CDC Cyber System. The function minimized in the least-squares refinement was:

$$\Sigma w(|F_o|-|F_c|)^2 \quad \text{where} \quad w=1/[(\sigma(F))^2+0.03F^2].$$

The discrepancy indices were $R_F=\Sigma||F_o|-(F_c)|/\Sigma F_o|$ and $R_{wF}=[\Sigma w(|F_o|-F_c|)^2/\Sigma|F_o|^2]^{1/2}$ and the "goodness of fit" is $[\Sigma w(|F_o|-|F_c|)^2/(m-n)]^{1/2}$. Neutral atom scattering factors and anomalous dispersion corrections for non-H atoms were used. The final positional parameters are collected in Table II. Listings of observed and calculated structure factors and anisotropic thermal parameters are available. *See* the note on supplementary material available at the end of this paper.

Crystal Data. – $C_{46}H_{35}O_9P_3Ru_4.CH_2Cl_2$, M.W. 1313.7, monoclinic space group $P2_1/n$, $a=17.046(2)$, $b=16.347(5)$, $c=17.870(3)$ Å, $\beta=87.02(1)°$, $U=4972.8$, $Z=4$. Four circle diffractometry, 2785 reflections $[I/\sigma(I)>3.0]$, anisotropic temperature factors for Ru, P, all CO groups and the CH_2Cl_2 molecule; phenyl groups isotropic, with H atoms placed in calculated positions and not refined; cluster H atoms refined isotropically; $R=0.038$, $R_w=0.056$ [13].

NMR data of $(\mu\text{-H})_4Ru_4(CO)_9$ (tripod)

^{1}H NMR

The variable temperature ^{1}H NMR spectra of $(\mu\text{-H})_4Ru_4(CO)_9$ (tripod) in the hydride region with CD_2Cl_2 : CHF_2Cl (1 : 1) as solvent are shown in Figure 1. From 30° to −60° the resonance remains essentially unchanged and appears as a sharp singlet ($\Delta\nu_{1/2}<1$ Hz) at τ 25.76. However, at higher resolution, this signal could be seen to have a narrow quartet structure with $J_{P-H}=0.5$ Hz, thus indicating that the rearrangement processes involved were indeed intramolecular. This small observed coupling constant is a result of the averaging of coupling constants of different sign (*vide infra*) and has been observed in related systems [5a, 6]. Below −60°, the hydride resonance can be seen to broaden and at −90° two broad signals, X and Y, of equal intensity emerge at τ 24.8 and τ 26.7. Below −100°, each signal is split into two resonances of equal intensity. Hence signals (at −100°) are found for X′ and X″ at τ 24.48 (*d*, $^2J_{P-H}=\pm28$ Hz) and τ 25.12 (*t*, $^2J_{P-H}=\pm14$ Hz) and for Y′ and Y″ at τ 26.44 (*d*, $^2J_{P-H}=\pm28$ Hz), and τ 27.00 (*d*, $^2J_{P-H}=\pm14$ Hz). Below these temperatures, no further

change is observed before crystallisation of the complex occurs. From this data, two intramolecular processes are occurring:

(*a*) Process *I* which occurs with a low activation energy which equilibrates the hydrides X′ and X″ at the same time as Y′ is equilibrated with Y″. From the coalescence temperature ($T_c = -95°$), the process occurs with an apparent $\Delta G_{173} = 8.2$ kcal.mol^{-1}. Alternatively measurement of the residual widening of the doublets (Y′, Y″) (~15 Hz) at $-120°$ gives $\Delta G_{153} = 7.5$ kcal.mol^{-1}.

(*b*) Process *II* which causes the exchange of X with Y and which from the coalescence temperature T_c ($-86°$) occurs with an activation barrier of $\Delta G_{187} = 8.3$ kcal.mol^{-1}.

The phenyl resonances of the tripod ligand, although complex in structure, show related changes. Hence at $-130°$, a broad multiplet (τ 2.0–4.0) is observed which on raising the temperature to $-110°$ becomes a relatively symmetric seven line pattern. This change appears to correspond to the occurrence of process I. Between $-100°$ and $-86°$, a further broadening occurs which can be associated with process II. However interestingly, from $-30°$ to $+30°$, further spectral changes occur and the resonances become considerably sharper, now occupying only the region τ 2.5-3.5. Although detailed analysis of these spectra has not been attempted, it appears a *third process* is occurring at higher energy which can be observed by changes in the phenyl resonances but does not affect the hydride or carbonyl (*see* below) spectra. We will discuss this point later.

^{13}C NMR

Variable temperature ^{13}C NMR spectra of the carbonyl region of a *ca.* 35% ^{13}CO enriched sample of $(\mu\text{-H})_4Ru_4(CO)_9$(tripod) at 62.86 MHz are depicted in Figure 2. At 30°, two resonances are observed with approximate relative intensities 6 : 3 at 196.8 and 191.7 p.p.m. respectively. The lower field singlet arises from the six radial carbonyl groups in the basal plane, the other resonance being assigned to the three apical carbonyl ligands and appears as a poorly resolved quartet ($^3J_{P-C} \sim 4$ Hz).

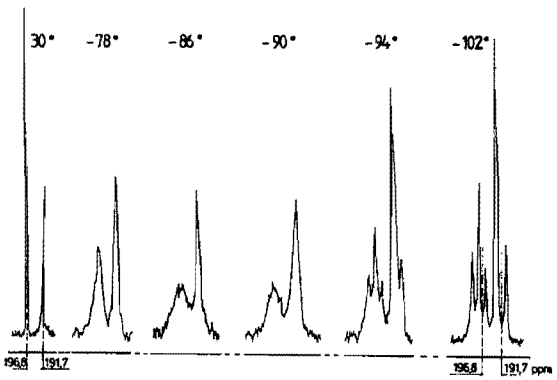

Figure 2. – Variable temperature ^{13}C{^{1}H} NMR spectra of the carbonyl region for $(\mu\text{-H})_4Ru_4(CO)_9$ (tripod), CD_2Cl_2 solution, 62.86 MHz.

Upon lowering the temperature to $-86°$, the signal of the radial carbonyls broadens considerably more than that of the apical set, so that at *ca.* $-90°$ the radial carbonyls are split into a 4 : 2 pattern, which overlap the somewhat broadened apical resonances, giving rise to two broad resonances (relative integrated intensities ~4 : 5). The splitting of the radial carbonyls into the 4 : 2 pattern at $-86°$ is in agreement with a free energy of activation of 8.3 kcal.mol^{-1}. Note that the broad lowfield peak is a partially resolved doublet (separation ~1.5 p.p.m.). Below $-94°$ the low field signal is now further split into a 1 : 2 : 1 pattern, whereas the upfield peak is now resolved into two resonances (4 : 1) which results from a 2 : 1 pattern of apical carbonyl resonances overlapping with two radial resonances. Hence the limiting spectrum can be assigned (on taking account of the weighted average of the peaks observed) as follows: (i) the six radial carbonyl groups give rise to four signals in the ratio 1 : 2 : 1 : 2 at 200.6, 198.6, 196.6 and 192.7 p.p.m. and (ii) the three apical carbonyls yield two singlets in a 2 : 1 ratio at 192.7 and 189.7 p.p.m.

^{31}P NMR

The ^{31}P {^{1}H} NMR of $(\mu\text{-H})_4Ru_4(CO)_9$ (tripod) in CD_2Cl_2 at 30° shows a narrow singlet at 35.9 p.p.m. (from H_3PO_4, $\Delta\nu_{1/2} \sim 5$ Hz). As the temperature is lowered, the resonance broadens at $-100°$, $\Delta\nu_{1/2} \sim 50$ Hz. No splitting of this signal was observed and no useful conclusions could be reached.

The spectroscopic data thus indicate (i) that tripod is indeed capping one face of the tetrahedral core, as evidenced particularly by the high temperature ^{13}C and ^{1}H spectra. (ii) that the four hydride ligands are non-equivalent at very low temperature but at intermediate temperatures a 2 : 2 pattern is observed consistent with core structure *A*. Two possibilities for this non-equivalence were considered: (*a*) the hydride ligands adopt the structure *A* except that as a result of the presence of the tripod ligand, were unsymmetrically

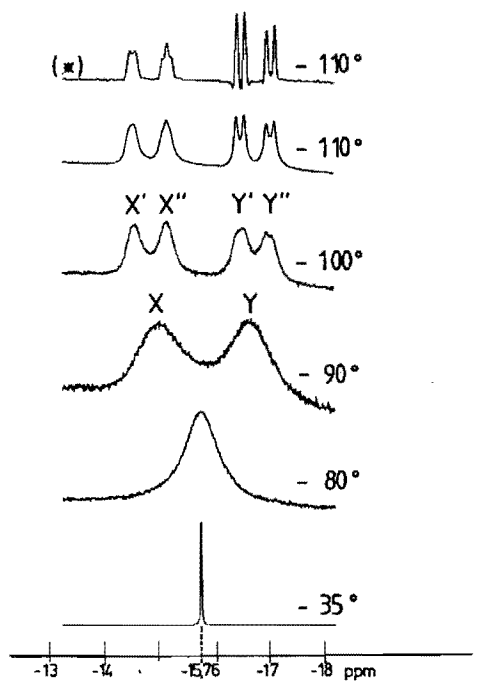

Figure 1. – Variable temperature ^{1}H NMR spectra of the metal hydride region for $(\mu\text{-H})_4Ru_4(CO)_9$(tripod), CD_2Cl_2/CHF_2Cl solution, 200 MHz. (*) Resolution enhancement by Lorentzian to Gaussian transformation (LB = −25 Hz, GB = 0.08).

bridging the Ru-Ru bonds or (*b*) the tripod ligand was complexed in an unsymmetrical fashion. A single crystal X-ray determination was carried out to clarify this problem. In the light of the solid state structural results, we will then discuss the structure and dynamics of this molecule in solution.

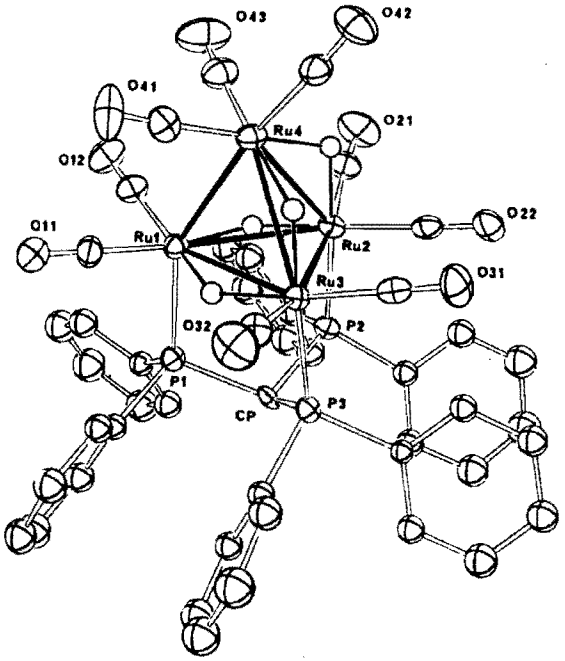

Figure 3. – The molecular structure of $H_4Ru_4(CO)_9$(tripod). Carbonyl carbons are named similarly to the oxygen atoms. Hydrides are named for the ruthenium atoms to which they are attached: they have been assigned arbitrary B values for this figure. The labelling of the phenyl rings may be found in Figure 4.

Description of the structure

Tables III and IV contain listings of selected distances and angles. Figure 3 depicts a general view of the molecule. As expected the tripod ligand is attached by one phosphorus to each ruthenium of one face, henceforth referred to as the base, of the tetrahedral cluster. The four bridging hydrides were found and are disposed on the cluster with local idealized D_{2d} symmetry [3], where two of them are on edges of the base. This is the arrangement assumed for $(\mu\text{-H})_4Ru_4(CO)_{12}$ [3], $(\mu\text{-H})_4Ru_4(CO)_{11}P(OMe)_3$ [4], and $(\mu\text{-H})_4Ru_4(CO)_{10}(PPh_3)_2$ [3] although the crystallographic studies did not permit location of the hydrides in those molecules with absolute certainty. As noted by Churchill *et al.* [6], the positions of the edge bridging hydrides can be further characterized with respect to the cluster faces. Table V gives the dihedral angles between cluster (3 Ru) faces and the planes of the Ru–H–Ru bridges. H 13 and H 23 are close to coplanar with the base, while H 24 and H 34 lie closer to planes Ru 1, Ru 2, Ru 4 and Ru 1, Ru 3, Ru 4. The local cluster symmetry is thus reduced to C_s, with the mirror plane containing Ru 1 and Ru 4 and between Ru 2 and Ru 3. The presence of the hydride ligands produces several distortions in the geometry of the compound: (*a*) the Ru–Ru distances bridged by hydrogen average 2.95 Å while those not bridged average 2.80 Å, in excellent agreement with previously reported data [5, 6]; (*b*) the group of 3 carbonyl bound to the apical Ru 4 are tilted away from bridging hydrides H 24 and H 34, thus the normal to the plane defined by O 41, O 42 and O 43 makes an angle of 165° with the plane defined by Ru 1, Ru 2 and Ru 3, and it lies close to the *pseudo* C_s mirror plane. A similar distortion is evident in the basal plane; the CO groups 21 and 32, near H 12 and H 13, make angles of 113.8(4) and 110.4(3)° with the Ru 1–Ru 2 and Ru 1–Ru 3 bonds respectively while CO groups 22 and 31 make angles of 88.6(3) and 93.5(3)° with the bond Ru 2–Ru 3, which is not bridged.

Table III. – Bond lengths (Å) and estimated standard deviations for $H_4Ru_4(CO)_9$ (tripod) CH_2Cl_2.

Atom 1 – Atom 2	Distance (esd)	Atom 1 – Atom 2	Distance (esd)
Ru 1 – P 1	2.336(3)	Ru 2 – P 2	2.316(3)
Ru 1 – C 11	1.84(1)	Ru 2 – C 21	1.91(1)
Ru 1 – Cl 2	1.85(1)	Ru 2 – C 22	1.83(1)
Ru 1 – Ru 2	2.964(1)	Ru 2 – Ru 3	2.819(1)
Ru 1 – Ru 3	2.948(1)	Ru 2 – Ru 4	2.913(1)
Ru 1 – Ru 4	2.770(1)	Ru 2 – H 12	1.46(7)
Ru 1 – H 12	1.56(7)	Ru 2 – H 24	1.76(10)
Ru 1 – H 13	1.73(9)		
Ru 3 – P 3	2.342(3)	Ru 4 – C 41	1.86(1)
Ru 3 – C 31	1.83(1)	Ru 4 – C 42	1.89(1)
Ru 3 – C 32	1.91(1)	Ru 4 – C 43	1.85(1)
Ru 3 – Ru 4	2.963(1)	Ru 4 – H 24	1.74(10)
Ru 3 – H 13	1.55(9)	Ru 4 – H 34	1.82(7)
Ru 3 – H 34	1.65(7)		
C 11 – O 11	1.17(1)	C 32 – O 32	1.13(1)
C 12 – O 12	1.17(1)	C 41 – O 41	1.15(1)
C 21 – O 21	1.15(1)	C 42 – O 42	1.14(1)
C 22 – O 22	1.18(1)	C 43 – O 43	1.16(2)
C 31 – O 31	1.17(1)		
CP – P 1	1.93(1)	CP – P 3	1.91(1)
CP – P 2	1.91(1)		
P 1 – C 111	1.83(1)	P 1 – C 121	1.84(1)
C 111 – C 112	1.41(2)	C 121 – C 122	1.39(2)
C 111 – C 116	1.37(2)	C 121 – C 126	1.38(1)
C 112 – C 113	1.45(2)	C 122 – C 123	1.41(2)
C 113 – C 114	1.31(2)	C 123 – C 124	1.32(2)
C 114 – C 115	1.39(2)	C 124 – C 125	1.38(2)
C 115 – C 116	1.38(2)	C 125 – C 126	1.42(2)
P 2 – C 211	1.81(1)	P 2 – C 221	1.84(1)
C 211 – C 212	1.38(2)	C 221 – C 222	1.39(2)
C 211 – C 216	1.38(2)	C 221 – C 226	1.38(2)
C 212 – C 213	1.39(2)	C 222 – C 223	1.40(2)
C 213 – C 214	1.34(2)	C 223 – C 224	1.36(2)
C 214 – C 215	1.34(2)	C 224 – C 225	1.37(2)
C 215 – C 216	1.43(2)	C 225 – C 226	1.39(2)
P 3 – C 311	1.85(1)	P 3 – C 321	1.83(1)
C 311 – C 312	1.37(1)	C 321 – C 322	1.39(2)
C 311 – C 316	1.41(1)	C 321 – C 326	1.42(1)
C 312 – C 313	1.39(2)	C 322 – C 323	1.40(2)
C 313 – C 314	1.37(2)	C 323 – C 324	1.37(2)
C 314 – C 315	1.38(2)	C 324 – C 325	1.35(2)
C 315 – C 316	1.37(2)	C 325 – C 326	1.40(2)
		The CH_2Cl_2 Molecule	
Cl – Cl 1	1.72(2) Å	Cl 1 – C – Cl 2	110(1)°
Cl – Cl 2	1.74(2)		

Table IV. – Selected angles in $H_4Ru_4(CO)_9$ (tripod) with estimated standard deviations in parentheses.

Atom 1	Atom 2	Angle (esd)	Atom 1	Atom 2	Angle (esd)	Atom 1	Atom 2	Angle (esd)	Atom 1	Atom 2	Angle (esd)	Atom 1	Atom 2	Angle (esd)
	Angles at Ru1			Angles at Ru2			Angles at Ru3			Angles at Ru4			Angles at P1	
RU2	RU3	56.96(3)	RU1	RU3	61.23(3)	RU1	RU2	61.81(3)	RU1	RU2	62.81(3)	RU1	CP	108.9(3)
RU2	RU4	60.94(3)	RU1	RU4	56.24(3)	RU1	RU4	55.90(3)	RU1	RU3	61.77(3)	RU1	C111	119.4(3)
RU2	C11	157.6(4)	RU1	C21	113.8(4)	RU1	C31	152.3(3)	RU1	C41	85.8(3)	RU1	C121	115.6(3)
RU2	C12	103.2(4)	RU1	C22	149.1(3)	RU1	C32	110.4(3)	RU1	C42	172.9(3)	CP	C111	104.9(4)
RU2	P1	94.27(8)	RU1	P2	88.49(8)	RU1	P3	92.67(7)	RU1	C43	89.7(4)	CP	C121	107.5(4)
RU2	H12	11(3)	RU1	H12	12(3)	RU1	H13	28(3)	RU1	H12	34(2)	C111	C121	99.5(3)
RU2	H13	81(3)	RU1	H24	88(3)	RU1	H34	86(3)	RU1	H24	95(3)		Angles at P2	
RU3	RU4	62.33(3)	RU3	RU4	62.23(3)	RU2	RU4	60.44(3)	RU1	H34	88(2)	RU2	CP	110.3(3)
RU3	C11	104.2(4)	RU3	C21	167.5(3)	RU2	C31	93.5(3)	RU2	RU3	57.33(3)	RU2	C211	120.1(3)
RU3	C12	156(4)	RU3	C22	88.6(3)	RU2	C32	168.0(3)	RU2	C41	147.5(4)	RU2	C221	115.1(4)
RU3	P1	90.82(7)	RU3	P2	95.52(8)	RU2	P3	88.46(7)	RU2	C42	112.7(4)	CP	C211	104.4(5)
RU3	H12	68(3)	RU3	H12	73(2)	RU2	H13	89(3)	RU2	C43	94.3(4)	CP	C221	107.4(5)
RU3	H13	25(3)	RU3	H24	82(3)	RU2	H34	85(3)	RU2	H12	30(2)	C2111	C221	98.2(5)
RU4	C11	100.9(3)	RU4	C21	105.3(3)	RU4	C31	102.1(3)	RU2	H24	33(3)		Angles at P3	
RU4	C12	98.7(4)	RU4	C22	105.5(3)	RU4	C32	107.8(3)	RU2	H34	79(2)	RU3	CP	110.9(3)
RU4	P1	150.12(8)	RU4	P2	143.81(8)	RU4	P3	142.76(8)	RU3	C41	101.7(4)	RU3	C311	117.6(3)
RU4	H12	62(2)	RU4	H12	58(3)	RU4	H13	72(3)	RU3	C42	111.3(4)	RU3	C321	118.7(3)
RU4	H13	76(3)	RU4	H24	33(3)	RU4	H34	33(3)	RU3	C43	145.9(4)	CP	C311	107.6(4)
C11	C12	91.9(5)	C21	C22	94.3(5)	C31	C32	91.6(5)	RU3	H12	61(2)	CP	C321	103.7(4)
C11	P1	98.2(4)	C21	P2	95.8(3)	C31	P3	99.6(3)	RU3	H24	78(3)	C311	C321	96.7(3)
C11	H12	163(3)	C21	H12	102(3)	C31	H13	171(3)	RU3	H34	30(2)		Angles at CP	
C11	H13	82(3)	C21	H24	87(3)	C31	H34	79(3)	C41	C42	97.6(5)	P1	P2	107.6(5)
C12	P1	103.5(4)	C22	P2	101,8(3)	C32	P3	101.4(3)	C41	C43	93.7(5)	P1	P3	107.9(5)
C12	H12	92(3)	C22	H12	159(3)	C32	H13	84(3)	C41	H12	120(2)	P2	P3	103.2(4)
C12	H13	170(3)	C22	H24	80(3)	C32	H34	85(3)	C41	H24	178(3)			
P1	H12	97(2)	P2	H12	90(3)	P3	H13	89(3)	C41	H34	92(2)			
P1	H13	85(3)	P2	H24	177(3)	P3	H34	173(3)	C42	C43	96.4(5)			
H12	H13	92(4)	H12	H24	88(4)	H13	H34	93(4)	C42	H12	142(2)			
									C42	H24	81(3)			
									C42	H34	85(2)			
									C43	H12	85(2)			
									C43	H24	88(3)			
									C43	H34	174(2)			
									H12	H24	61(4)			
									H12	H34	90(3)			
									H24	H34	86(4)			

Figure 4. – wed from b numbered c

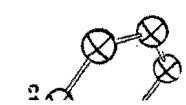

Table V. –

Plane 1	
Ru1, Ru2,	
Ru1, Ru2,	
Ru1, Ru3,	
Ru1, Ru3,	
Ru2, Ru4,	
Ru2, Ru4,	
Ru3, Ru4,	
Ru3, Ru4,	

As men
spectra are
try we exar
of further
tripod liga
rings are o
metry to (
chiral, the
arrangemer
to avoid a
the radial
took place
2.0 Å of t
oriented pe
Waals cont
cannot orie
steric inter
ture (Figur
wise, quasi

Table V. – Cluster dihedral angles in $H_4Ru_4(CO)_9$ (tripod).

Plane 1	Plane 2	Dihedral angle (°)
Ru1, Ru2, H12	Ru1, Ru2, Ru3	170
Ru1, Ru2, H12	Ru1, Ru2, Ru4	84
Ru1, Ru3, H13	Ru1, Ru2, Ru3	171
Ru1, Ru3, H13	Ru1, Ru3, Ru4	62
Ru2, Ru4, H24	Ru2, Ru3, Ru4	122
Ru2, Ru4, H24	Ru1, Ru2, Ru4	166
Ru3, Ru4, H34	Ru2, Ru3, Ru4	134
Ru3, Ru4, H34	Ru1, Ru3, Ru4	152

As mentioned above, since the low temperature NMR spectra are more complex than would result from C_s symmetry we examined the solid state structure for a possible source of further disymmetry. Figure 4 shows a bottom view of the tripod ligand and basal ruthenium atoms. The six phenyl rings are oriented helically, thus reducing the molecular symmetry to C_1 in the solid state. We see that the cluster is chiral, the source of the chirality arising from the propeller arrangement of phenyl groups. This arrangement is adopted to avoid a severe steric interaction of the phenyl group with the radial carbonyl above. Thus, unless angular distortion took place, the ortho-hydrogen atoms would be within *ca.* 2.0 Å of the CO carbon atoms if the phenyl groups were oriented perpendicular to the basal Ru 3 plane. A Van der Waals contact would be *ca.* 3.0 Å. Further the phenyl groups cannot orient parallel to this basal plane because of strong steric interactions between themselves. Interestingly the structure (Figure 4) also shows the phenyl groups are in a pairwise, quasi-parallel arrangement.

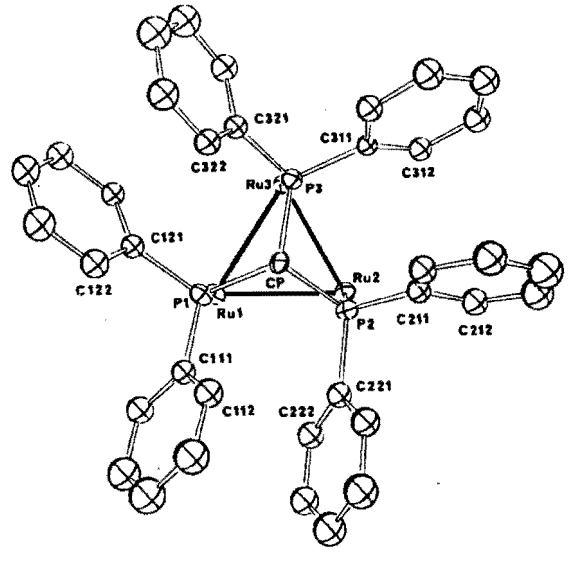

Figure 4. – The Ru_3(tripod) fragment of $H_4Ru_4(CO)_9$(tripod) viewed from below relative to Figure 3. The phenyl carbon atoms are numbered consecutively.

Discussion of the structure and dynamic behavior of $(\mu\text{-H})_4Ru_4(CO)_9$(tripod) in solution

We see that the chiral nature of $(\mu\text{-H})_4Ru_4(CO)_9$(tripod) observed in the solid state is clearly preserved in solution. Hence four separate signals for the hydride ligands are observed, two being approximately *trans* to the phosphorus nuclei with large and closely similar coupling constants ($^2J_{P-H} \sim \pm 28$ Hz, *see* $H_4Ru_4(CO)_{10}$(diphos)) and two hydrides *cis* to the phosphine ligand ($^2J_{P-H} \sim \pm 14$ Hz). The observed chemical shift difference arises from the relative positions of the hydrides to the anisotropic ring current provided by the helical array of phenyl groups. We see that the ground state (limiting) structure should show in principle all nine CO groups different in the ^{13}C spectrum whereas a 1 : 2 : 1 : 2 (radial) and 2 : 1 (apical) pattern is observed. The ^{13}C spectrum (or the spectrometer) is thus less sensitive to the asymmetry in the molecule, leaving some degeneracy. We now discuss the three dynamic processes observed by NMR.

PROCESS I

This lowest energy process is seen to (i) equilibrate pairwise the four hydride ligands and (ii) simplify the ^{13}C carbonyl spectrum greatly. The movement most consistent with these observations is the conversion of one enantiomer into the other by a restricted rotational movement of the phenyl groups. This is shown schematically (*see* Scheme II). This involves passage of the ortho-protons of the phenyl groups by the radial CO groups and this librational (or oscillatory) motion involves simply a 30-40° rotation about the phosphorus-carbon bond. Although we have no direct evidence it would seem that this racemisation process involves a correlated six-ring motion. This process generates a mirror plane, and hence the pairwise equilibration of the hydride ligands. The ^{13}C carbonyl spectrum pattern that is observed (4 : 2 radial; 3 apical) is different from that strictly anticipated (2 : 2 : 2 radial; 2 : 1 apical) but note that the broad low field resonance is apparently split into two resonances (Figure 2). The reason for the equivalence of the apical carbonyls remains speculative but possibly, as found for analogous systems [1], a concomitant three fold rotational motion is occurring at the apical Ru.

We note also that no motion of the hydride or carbonyl ligands alone can explain these spectral changes.

PROCESS II

This intermediate energy process causes complete equilibration of the hydride ligands [11] as well as the radial and, separately, the apical carbonyl ligands. This is the classical hydride migration process about a cluster surface, which has been studied in some detail [5, 6] previously. We have little

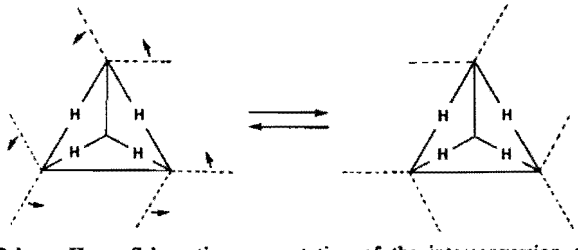

Scheme II. – Schematic representation of the interconversion of enantiomers by a concerted librational motion of phenyl groups (------).

more to add in this study, except that any migration process envisaged (edge-face-edge or edge-terminal-edge scrambling pathway) must in this case lead to occupation of all edges of the tetrahedron. The simplest pathway would involve passage via structure *B* although other mechanisms are also conceivable.

PROCESS III

This process is observed only at higher temperatures in the phenyl resonance patterns. We believe this to involve a *full* rotation of the phenyl groups. This molecule thus falls into a class of molecular propellers [12], but given the steric crowding involved it would seem here that the ring flip order is probably low.

Acknowledgements

We thank the GRECO-CO for partial support of this work. Continuing support by the C.N.R.S. (E.R.A. 721) and the National Science and Engineering Research Council of Canada (PHB, U.S.) are also gratefully acknowledged.

Supplementary material available

Tables of observed and calculated structure factors and thermal vibration parameters (22 pages). Ordering information is given on any current masthead page.

REFERENCES AND NOTES

[1] A. A. Bahsoun, J. A. Osborn, C. Voelker, J. J. Bonnet, and G. Lavigne, *Organometallics*, **1**, 1114 (1982).
[2] A. A. Arduini, A. A. Bahsoun, J. A. Osborn, and C. Voelker, *Angew. Chem. Int. Ed. Engl.*, **19**, 1024 (1980).
[3] R. D. Wilson, S. M. Wu, R. A. Love, and R. Bau, *Inorg. Chem.*, **17**, 1271 (1978).
[4] *See* footnote 24: R. D. Wilson, and R. Bau, *J. Amer. Chem. Soc.*, **98**, 4687 (1976).
[5] (*a*) J. R. Shapley, S. I. Richter, M. R. Churchill, and R. A. Lashewysz, *J. Amer. Chem. Soc.*, **99**, 7384 (1977); (*b*) M. R. Churchill, and R. A. Lashewysz, *Inorg. Chem.*, **17**, 1950 (1978).
[6] M. R. Churchill, R. A. Lashewysz, J. R. Shapley, and S. I. Richter, *Inorg. Chem.*, **19**, 1277 (1980).
[7] S. A. Knox, J. W. Koepke, M. A. Andrews, and H. D. Kaesz, *J. Amer. Chem. Soc.*, **97**, 3942 (1975).
[8] D. F. Grant, and E. J. Gabe, *J. Appl. Cryst.*, **11**, 114 (1978).
[9] E. J. Gabe, A. C. Larson, F. L. Lee, and Y. Wang, *The NRC PDP-8 e Crystal Structure System*, NRC, Ottawa (1979).
[10] *International Tables for X-Ray Crystallography*, Kynoch Press, Birmingham, England, Vol. IV, Tables 2.28, 2.31 (1975).
[11] The reason for the very small observed coupling in the averaged hydride spectrum is now evident. If $^2J_{(P-H)cis} \sim 1/2\,^2J_{(P-H)trans}$ and are of opposite signs it can be shown $^2J_{P-H}(\text{average}) = 1/6[2J_{(P-H)cis} + J_{trans}]$ which is close to zero.
[12] *See* K. Mislow, *Acc. Chem. Res.*, **9**, 27 (1976).
[13] Supplementary material for this work is available on request from the authors. Any request should be accompanied by a full literature citation for this communication.